49th AIAA Aerospace Sciences Meeting including the New Horizons Forum and Aerospace Exposition
4 - 7 January 2011, Orlando, Florida

AIAA 2011-274

A Modern Compressible Flow Laboratory Experience for Undergraduates

Frank K. Lu,[*] Sikander Ali,[†] Eric M. Braun,[‡] and Luca Maddalena[§]

University of Texas at Arlington, Arlington, Texas, 76019

Two experiments involving compressible flow, namely, unsteady flow in a shock tube and expansion in a freejet, are described. The latter includes experience in numerical simulations. These laboratory experiences reinforce classroom instruction and serve a number of learning goals. By including simulations and a simple inviscid model, the data from the freejet experiments can be validated and verified. Such a process is increasingly important for engineers.

I. Introduction

A WELL-DEVELOPED laboratory experience is an important aspect of any undergraduate engineering curriculum, including aerospace engineering. The aerospace laboratory follows a basic measurements course which typically includes digital data acquisition techniques, instrumentation, data processing and elementary statistics. At the authors' institution, the basic sophomore measurements course is then followed consecutively by an aero-structures and an aerodynamics laboratory in the fall and spring semesters of the junior year. The students by the spring semester of the junior year will have taken an incompressible aerodynamics course. They will be enrolled in the compressible aerodynamics course concurrently with the aerodynamics laboratory. Thus, a compressible laboratory experience in the same semester will help to reinforce classroom instruction.

Unlike the basic measurements course, reinforcing classroom instruction imposes a different set of objectives for the aerodynamics laboratory. A critical objective is to ensure that students understand the physics of the flow which is in all likelihood more complicated that the idealizations introduced in the classroom. Thus, a part of this objective is to allow the students to perform a critical evaluation of inviscid theory. For example, the presence of shocks in a nozzle induces boundary layer separation will likely not be well explained in class. Nonetheless, it is important to ensure that the students are aware of the limitations of inviscid theory in situations where viscous effects are important.

A separate challenge which may have not been well addressed in laboratory development is exposing students to modern engineering software tools. Some may argue against introducing such tools in an academic environment for fear that these tools defeat the learning process. Others argue that software can mislead students into thinking that these tools can solve problems and lull them into a sense of complacency where the danger of erroneous results are not appreciated and thus "sanity" checks are not made. Nonetheless, a

---

[*]Professor and Director, Aerodynamics Research Center, Department of Mechanical and Aerospace Engineering, Box 19018. Associate Fellow AIAA.

[†]Undergraduate Research Assistant, Aerodynamics Research Center, Department of Mechanical and Aerospace Engineering, Box 19018. Student Member AIAA.

[‡]Graduate Research Associate, Aerodynamics Research Center, Department of Mechanical and Aerospace Engineering, Box 19018. Student Member AIAA.

[§]Assistant Professor, Aerodynamics Research Center, Department of Mechanical and Aerospace Engineering, Box 19018. Member AIAA.

American Institute of Aeronautics and Astronautics

well-controlled use of software, as we propose here, can help to reinforce certain skills, such as the need for sanity checks: the so-called validation and verification. Thus, the laboratory environment may be an excellent one for integrating experiment, modeling and theory, an approach that is increasingly expected in modern engineering practice. Finally, once some experience is gained, software tools help greatly in engineering design. Toward this goal, the commercial fluids solver, FLUENT$^{\circledR}$, is introduced into the aerodynamics laboratory experience.

To meet the objectives of (i) improving the understanding of compressible flow, (ii) application of theory to experiment, (iii) validation and verification, and (iv) use of software, two compressible flow experiments were developed. Other secondary objectives include typical ones of an experimental course, such as understanding the characteristics of instruments, data acquisition, data analysis, including uncertainty analysis, and report writing.

The two experiments are based on a shock tube for teaching unsteady compressible flow and a supersonic nozzle/free jet with its inherent versatility. The shock tube is easy and inexpensive to develop, using mostly off-the-shelf components with a minimum amount of machining. The nozzle can be used to study underexpanded, perfectly expanded and overexpanded free jets. It can also be used to study nozzle off-design performance at low Mach number, with internal shocks inducing boundary layer separation. The nozzle experiment is complemented with numerical simulations. The nozzle was deliberately constructed with a rectangular cross section so that it can be operated as a miniature supersonic tunnel. Thus, small models can be mounted in the test section to provide further experiences. The nozzle experiment is more elaborate and expensive, even though every effort was made to use off-the-shelf components.

II. Implementation

The shock tube and the free jet facilities are housed in a research laboratory. While these facilities occupy some space, the execution of the experiments has a minimal impact on research activities. The experiments take up only two weeks, requiring preparation by the teaching assistants and the laboratory technician. The preparations include checking the instrumentation, ensuring that all plumbing and wiring are working properly. The experiments also require the temporary use of data acquisition systems that would otherwise be used for research, and require checking that the data acquisition programs are operating properly. These checks may require a test run or two ahead of the actual laboratory sessions. Due to safety concerns, these laboratories are operated by the teaching assistants.

A.   Shock Tube

Specific objectives of this experiment are

- To develop an understanding of unsteady wave processes in a gas,

- To compute the shock Mach number from experimental data and compare against theory.

The shock tube experiment can be set up with low cost and ease, with a small amount of machining. Even though unsteady wave processes are not covered in the present classroom curriculum, this experiment provides exposure to compressible phenomena. It also provides understanding of shock and expansion processes, with the noteworthy distinction that compression can occur over a steep front, namely, a shock, whereas expansion is an isentropic process that occurs over an extended distance.

1.   Facility Description

The shock tube is shown schematically in Fig. 1(a) and a photograph is shown in Fig. 1(b). It consists of a high-pressure, driver section (right side) and a low-pressure, driven section (left side), both made of seamless, commercial steel pipe with an internal diameter of 1 in. The driver and driven tubes are 20 in.

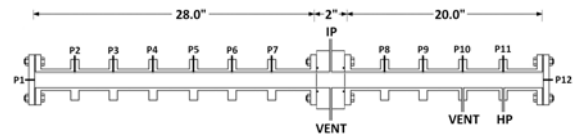American Institute of Aeronautics and Astronautics

and 28 in. long, respectively. While the driver tube is capped at its end, the driven tube is operated either capped or open to the ambient. Connecting the two tubes is a double diaphragm section, also made of steel. It is a 2-in. chamber. Diaphragms made of kitchen foil are placed on either side of the chamber. Next, the flanged ends of the driver and driven tubes are bolted to the double diaphragm section. A tight seal is obtained by including O-rings on the flange faces. The double diaphragm section makes it easy and safe to operate the shock tube. High-frequency pressure transducers (PCB Model 111A24) are mounted along the sides of the driver and driven tubes at a spacing of 4 in. Transducers are also mounted onto the end flanges of these tubes. The transducers are rated for a maximum pressure of 1000 psi. Although the 1000 psi rating is far above what was measured with this experiment, the high pressure transducers were selected for their ruggedness since the aluminum foil diaphragms usually burst into fragments during operation. The shock tube is shown schematically in Fig. 1(a) and a photograph is shown in Fig. 1(b). It consists of a high-pressure, driver section (right side) and a low-pressure, driven section (left side), both made of seamless, commercial steel pipe with an internal diameter of 1 in. The driver and driven tubes are 20 in. and 28 in. long, respectively. While the driver tube is capped at its end, the driven tube is operated either capped or open to the ambient. Connecting the two tubes is a double diaphragm section, also made of steel. It is a 2-in. chamber. Diaphragms made of kitchen foil are placed on either side of the chamber. Next, the flanged ends of the driver and driven tubes are bolted to the double diaphragm section. A tight seal is obtained by including O-rings on the flange faces. The double diaphragm section makes it easy and safe to operate the shock tube. High-frequency pressure transducers (PCB Model 111A24) are mounted along the sides of the driver and driven tubes at a spacing of 4 in. Transducers are also mounted onto the end flanges of these tubes. The transducers are rated for a maximum pressure of 1000 psi. Although the 1000 psi rating is far above what was measured with this experiment, the high pressure transducers were selected for their ruggedness since the aluminum foil diaphragms usually burst into fragments during operation.

Figure 1(a) shows the vents used both for safety and draining the intermediate section pressure. Intermediate and high-pressure lines are labeled by IP and HP respectively. High and intermediate pressure air are brought into the tube sections with solenoid valves manually triggered from the control room. The bank of solenoid valves is visible in the lower right of Fig. 1(b). The air is regulated so the IP fills first. Next, the HP is switched on. A third solenoid valve is used to vent the IP section to cause the double diaphragms to burst. A fourth solenoid valve is available to vent the HP section if necessary. The high-pressure air is introduced to the shock tube from a 175 psi compressor.

(a) Schematic of the shock tube along with the pressure transducer and filling arrangement.
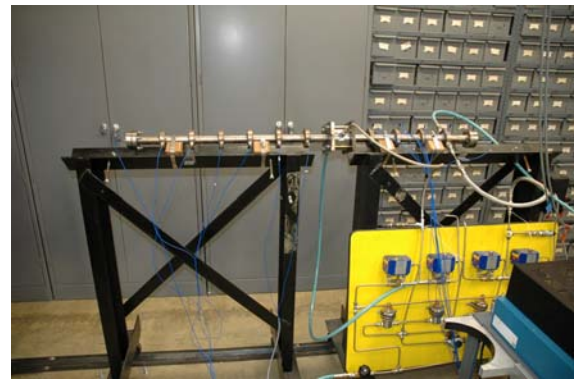
2. Test Protocol

As mentioned above, preparation for the laboratory includes instrumenting the shock tube with pressure transducers and connecting them to a high-speed data acquisition system with a LabVIEW® interface. Groups of 4–6 students witness the experiment from a control room.

Aluminum foil is placed on both sides of the double diaphragm section. The driver and driven sections are then bolted to the double diaphragm section, ensuring that there is a good seal between the sections. The diaphragm for this laboratory is constructed of several aluminum foil layers such that it will burst for a Δp of 110–130 psi. The

(b) Photograph of shock tube.

Figure 1. Shock tube.

intermediate, double-diaphgram section can be filled with air to 60 psig initially, which the diaphragms will safely hold. When the driver section is then filled to 150 psig, the Δp values across each diaphragm are still below their burst limit. The intermediate section is then exhausted quickly by activating a pressure relief vent. Activation of the vent causes Δp to rise sufficiently to burst the diaphragms. Bursting of the diaphragms starts the unsteady wave process in the shock tube. Before the vent is actuated, the DAQ and LabVIEW® program are started with an analog trigger that waits for a pressure rise of about 10 psi in transducer P7. Data are acquired for a half second. A similar experiment is performed with the driven tube uncapped.

3. Project Requirements

Data from the experiment are stored in EXCEL files for the students to analyze. Examples of the plotted data collected at a 100 kHz/channel, simultaneous sampling rate are shown in Fig. 2. The students are required to determine the time-of-flight τ from the data. Here, they will understand the practical difficulties of resolving a step pressure rise due to transducer size, sampling rate and noise. Once τ is determined, given the transducer spacing of x, the shock propagation speed and the Mach number can be computed:

$$u_s = x/\tau \qquad (1)$$
$$M_s = u_s/a_1 \qquad (2)$$

where the speed of sound $a_1 = \sqrt{\gamma R T_1}$. Students are required to perform an uncertainty analysis on their estimate of u_s and M_s since these values can be calculated 5–6 times depending on the mode of operation. The students also estimate the pressure ratio across the propagating shock p_2/p_1 which is an important parameter in shock tube performance. This pressure ratio is in fact related to the shock Mach number:

$$M_s = \sqrt{\frac{\gamma + 1}{2\gamma}\left(\frac{p_2}{p_1} - 1\right) + 1} \qquad (3)$$

Therefore, a separate calculation of M_s is obtained. The students also have to perform an uncertainty
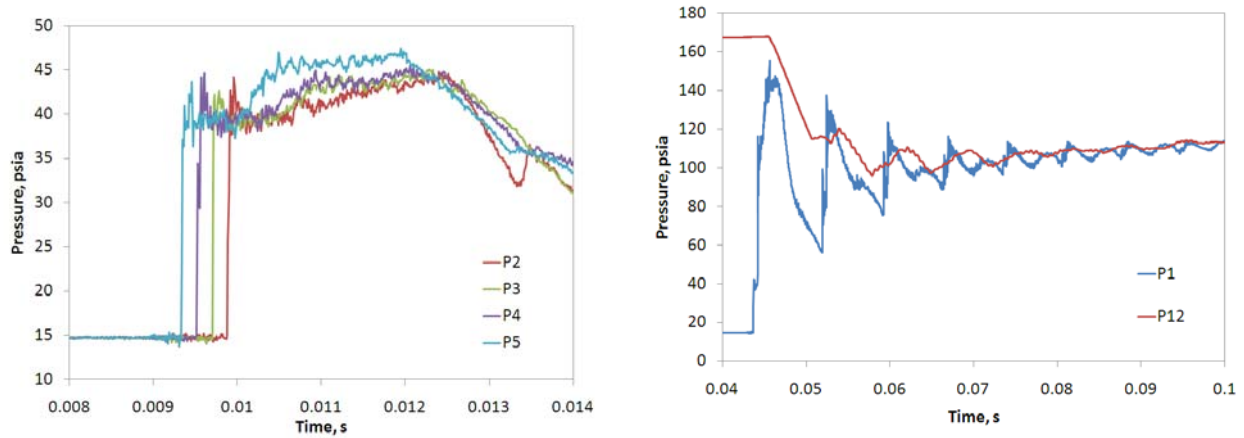
(a) Sample data with open driver tube.

(b) Sample data with closed driver tube.

Figure 2. Example of shock tube data.

analysis here, which is a little bit more involved. From the shock pressure ratio, the students can back

American Institute of Aeronautics and Astronautics

calculate the initial pressure ratio.

$$\frac{p_4}{p_1} = \frac{p_2}{p_1} \left\{ 1 - \frac{(\gamma - 1)\,(p_2/p_1 - 1)}{\sqrt{2\,\gamma\,[2\,\gamma + (\gamma + 1)\,(p_2/p_1 - 1)]}} \right\}^{-2\,\gamma/(\gamma-1)} \qquad (4)$$

The students are required to compare their computed value of p_4/p_1 against the measured one and comment on the results. The procedure is undertaken for the two test cases: open and closed end. The time-of-flight calculations are usually associated with an uncertainty of less than 10% of the value. However, uncertainty in the p_2/p_1 estimate and its associated p_4/p_1 and M_s values usually is greater than 10%. Comparing these calculation procedures and making a determination why one may be better to use over another reflects situations that will often be encountered by a practicing engineer.

Finally, the students construct an x–t diagram with the closed end data for the incident shock and the first reflection. The uncertainty from the wave speeds is also indicated in the diagram. If any errors are made while calculating the shock speed and its uncertainty, they should be obvious in the diagram and allow the student to see where errors have been made.
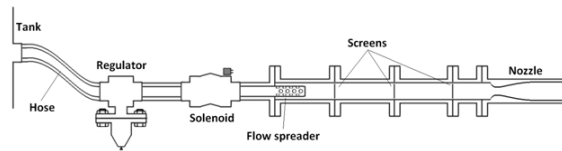
B. Free Jet

Specific objectives of this experiment are

- To understand the operation of a supersonic nozzle with a constant backpressure (or variable supply pressure)

- To observe the formation of an underexpanded, perfectly expanded and overexpanded free jet, including the wave patterns that are not ideal but regularly occur in practice.

- To observe shock formation in a severely overexpanded jet

To fulfill these objectives, a small facility featuring a nominal Mach 2, convergent-divergent nozzle was developed. This nozzle exhausts to the ambient which allows for observations of the freejet.

1. Design

The supersonic wind tunnel for the undergraduate laboratory experience was designed with several considerations. First, the students should have exposure to all of the different flow regimes that occur while the pressure ratio is varied between the stagnation and ambient conditions of the converging-diverging (CD) nozzle. The recognizable under- and over-expanded regimes with their shock diamond patterns can be readily visualized. A pressure scanner is used to measure the pressure in taps located along the nozzle contour. The tunnel sections leading up to the nozzle were deliberately sized such that a simple regulator could be used to control the plenum pressure. This arrangement proved to work well and obviated the need for a more elaborate control valve and large settling chamber.

(a) Schematic of supersonic freejet facility.

(b) Photograph.

Figure 3. The supersonic free jet.

American Institute of Aeronautics and Astronautics

The nozzle Mach number was arbitrarily selected to be 2. The selected run time was 20–30 s. This is more than adequate for gathering data from the pressure scanner and for obtaining schlieren movies. The nozzle throat is 1.4 in. high × 0.6 in. wide. This rectangular cross-section design allowed for the walls of the nozzle to be constructed of Lexan sheets for further flow visualization.[a] The height of the nozzle increases to 2.36 in. which matches with the size of the in-house schlieren system.[1]

The CD nozzle was designed using the method of characteristics without boundary layer corrections. One of the goals of the laboratory is to help students understand the importance of viscous effects that will cause a reduction of both the area ratio and the Mach number. After the area expansion, the nozzle contains a straight section which could be prepared in the future for inserting test articles. The bottom nozzle contour has 16 ports with a diameter of 0.0465 in. for use with a 16-channel, Esterline 9116 pressure scanner. Eleven ports are placed in the throat section to measure the pressure variation with area, and five ports are located in the test section.

A blowdown type, free jet tunnel configuration satisfies all of the criteria above for testing the nozzle. Run times can be predicted using a simple approach outlined by Pope and Goin[2] so as to size the storage tube. A storage tank with a 50 ft^3 volume and 400 psig pressure limit was selected for this facility.

The required pressure ratio for perfect expansion is $p_0/p_\infty = 7.84$, so p_0 must be set to at least 115 psia. A Jordan Valve Mark 60 sliding gate regulator that can maintain up to $p_0 = 175$ psia was chosen for this facility. The facility is started with a Granzow high mass flow solenoid valve. A schematic, not to scale, is shown in Fig. 3(a). The storage tank, filled by a 2000 psi compressor source, is connected to the sliding gate valve via a 2-in. high-pressure hose. Pipe sections connect to the valves up to the flow spreader location. At that location, a flange assembly was designed to connect the pipe to a 2.5 × 2.5 in. square section.

A flow spreader containing 24 radial ports that send air into a plenum chamber up to the nozzle throat, as can be seen in Fig. 3(a). Immediately downstream of the flow spreader are three 12-in. long flanged sections, each of which contains a mesh screen to reduce turbulence. The mesh sizes are 30, 40 and 50 with a solidity of about 45%. From the area ratio of the plenum chamber to the throat, air speed in the plenum chamber is less than 100 ft/s, which essentially means that stagnation conditions are upheld. The small flanged section between the last screen and the nozzle reduces the cross-sectional area from 2.5 × 2.5 in. to 2.5 × 0.6 in.

2. Simulation and Analytical Requirements

To expand the learning experience from merely experimental observations, the students will be exposed to a guided experience in using FLUENT® for flow simulation. The students enrolled in this course are presumed to have no experience with computational fluid dynamics. Consequently, the simulation given to the students to work with is finished with the exception of the commands that must be entered into FLUENT® to start a solution. Such an assignment may be considered a "canned" one because simply running it may not enhance basic understanding of computational fluid dynamics algorithms.[3]

There are several reasons why running the program as part of this laboratory assignment can be a good educational experience. First, students can understand how to use CFD to properly support experimental results (and vice versa). After running the FLUENT® program for several different stagnation pressure values, the pressure distribution along the centerline can be extracted to map p/p_0 for all of the flow conditions that can occur with a CD nozzle.[4] Figure 4(c) shows several of these conditions. The pressure distribution from the nozzle wall can also be matched with the pressure scanner data.

A second educational outcome from incorporating numerical simulation is to help develop an ability to understand any limits that exist with the FLUENT® model as compared to the experiment. The grid spacing has been left coarse so each solution converges in a few thousand iterations. Consequently, the shock and expansion wave patterns seen in the experiments cannot be replicated with this model. Even with finer grid spacing, the two-dimensional nozzle model can differ significantly from three-dimensionality in the experiment.
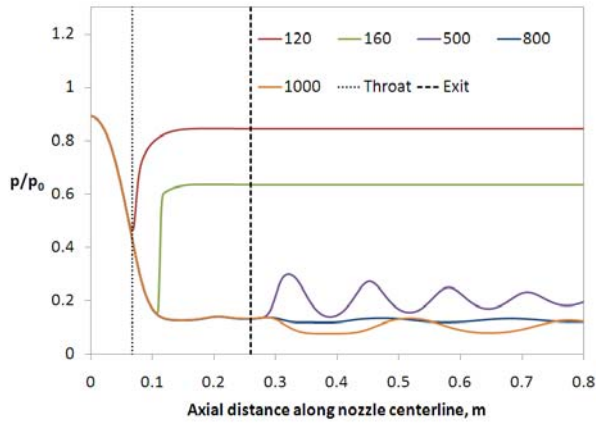
---

[a]Subsequent schlieren visualization revealed stress patterns in tightening the Lexan walls. These walls will be replaced by schlieren-quality glass.

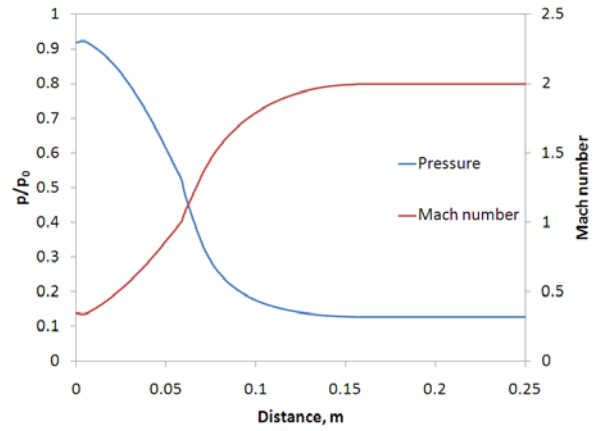American Institute of Aeronautics and Astronautics
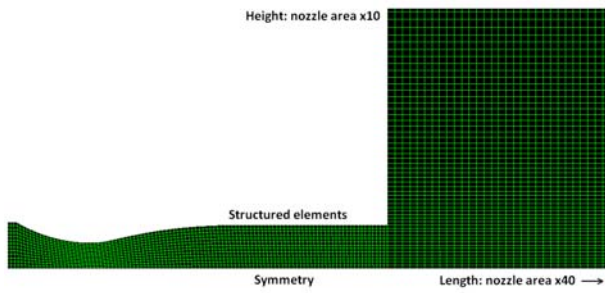
(a) Close-up view of solution domain.
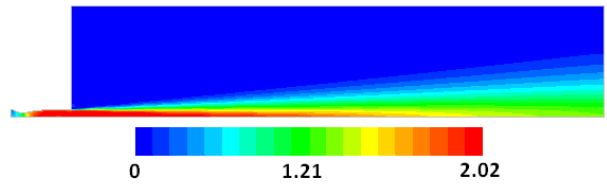
(b) Mach number contours of the perfectly expanded case.

(c) Centerline p/p_0 distribution for several nozzle states.

(d) Analytical Mach and pressure distributions.

Figure 4. Results from computational and analytical solutions.

Figure 4(a) shows a partial view of the solution domain. In order for the free jet simulation to converge properly, the length of the domain is about 20 times larger than the nozzle exit area (after accounting for the symmetry condition along the nozzle centerline). The pressure inlet, pressure outlet, and wall boundary conditions are used for the rest of the solution domain. About 40,000 structured cells are used, whereby overall size increases away from the nozzle and predicted exit plume location. A density-based, implicit, two-dimensional planar solution method is used. A standard k–ε viscous model is used with the constants provided by FLUENT® along with first-order upwind discretization. Other techniques could clearly be utilized for a more accurate solution, but they are not necessary for the current learning objectives. The students are given step-by-step instructions for setting boundary conditions, initializing the solution, monitoring convergence, and collecting results. Convergence is considered to be reached when the drag on the nozzle wall becomes constant along with residual values of 1e–6 or less.

Figure 4(d) shows the analytical solution for p/p_0 and M in the nozzle using isentropic flow equations.

$$\frac{p_0}{p} = \left(1 + \frac{\gamma - 1}{2}M^2\right)^{\gamma/(\gamma-1)} \tag{5}$$

$$\frac{A(x)}{A^*} = \frac{1}{M}\left[\frac{2}{\gamma + 1}\left(1 + \frac{\gamma - 1}{2}M^2\right)\right]^{(\gamma+1)/2(\gamma-1)} \tag{6}$$

In the isentropic equations, the geometry of the nozzle is used to first calculate the area ratio along the nozzle $A(x)/A^*$. The pressure ratio and Mach number are then computed using an iterative process for each point specified along the nozzle.

3. Experimental Results

The tunnel and data collection program are initiated by the teaching assistants from the control room. As for the shock tube experiment, groups of 4–6 students witness the experiment. Once the storage tank has been filled, the solenoid valve is simply switched on to start. The schlieren system and video camera can be turned on during the filling process. Once the nozzle is started, the regulator valve holds reasonably steady pressure for about 10 s. This pressure is held high enough such that the nozzle will remain overexpanded during that time. Once the regulator can no longer hold constant pressure, the pressure of the storage tank as it drains is essentially the stagnation pressure. Such behavior is typical of blow-down wind tunnels, and the control valve is usually shut at this point to conserve air. In the present case, it is left open and the nozzle progresses through all of the states based on pressure ratio.
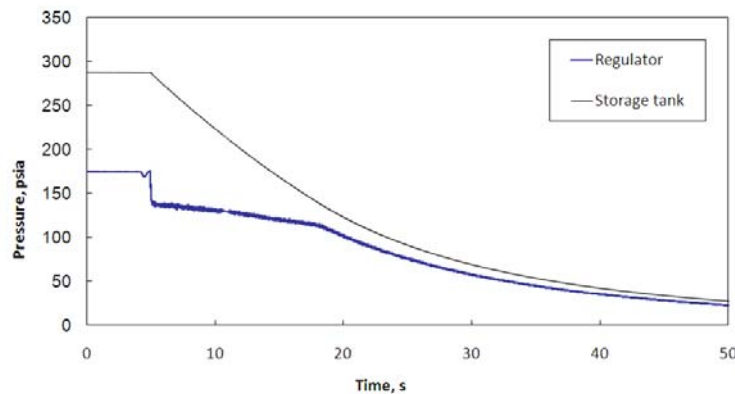
Figure 5. Storage tank and regulator/plenum pressures during a typical test.

American Institute of Aeronautics and Astronautics

Figure 6 shows several schlieren photographs taken of different nozzle states during a test. Photograph A was taken during the beginning of the test, where the nozzle flow is mildly underexpanded. The flow is characterized by expansion waves that reduce the nozzle exit pressure to the ambient pressure. Between the under- and overexpanded states, the shock and expansion waves nearly disappear when the nozzle passes through the perfectly expanded state shown in photograph B. After the perfectly expanded state, shocks stemming from the edge of the nozzle appear and reflect off each other. The pattern formed first appears to be similar to photograph A, but Mach stems and triple intersections quickly form as the oblique shock strength decreases. The triple point pattern is shown with both a knife-edge and color schlieren technique in photographs C and D.

Mathematically, the pressure ratio for which the shock wave will be located directly at the exit of the nozzle can be calculated easily. However, the constant area section at the end of the nozzle creates non-ideal flow patterns that are more likely to occur with practical devices like high-speed engines. When the pressure ratio drops to this condition, a normal shock enters the constant area section. Because of its strength, the boundary layer separates and forms a repeated lambda shock pattern that continues out and interacts with the shear layers. Photograph E shows the flow pattern at the beginning of this process. The shock structure then becomes extremely unstable for a few seconds until the shocks are entirely within the constant area section as shown in photograph F. Using the static pressure port data, one can calculate the pressure before and after the shock train and find that it is equal to the pressure ratio across a single normal shock. The shock train pattern then approaches the nozzle throat until the flow is entirely subsonic. The transition from choked to subsonic flow is indicated with a distinct change in sound.

These observations should prove to be useful for students because they provide a context for topics discussed in the propulsion course. For example, nozzle losses due to imperfect expansion should be well understood since all of the expansion states have been clearly observed in the lab. The unsteadiness observed as the shock wave pattern passed into the constant area section shows the difficulty of building an engine that can successfully control supersonic internal flow. For off-design conditions where the pressure ratio is not optimal, such unsteady conditions must be avoided. While the exit area ratio is fixed for this nozzle, aircraft engine nozzles can vary the area ratio so long as the p/p_0 ratios result in steady flow.

While the schlieren images are useful in aiding students to understand the behavior of the nozzle, the lab report assignment consists mainly of comparing the experimental, computational, and analytical results. Data are collected at a rate of 2 Hz for each of the pressure taps along the nozzle. The stagnation pressure can be calculated using data from the pressure tap located at the nozzle throat assuming a Mach number of one.

$$P_0 = p_{throat} \left(1 + \frac{\gamma - 1}{2} 1^2 \right)^{\gamma/(\gamma-1)} \tag{7}$$

$$M_i = \sqrt{\frac{2}{\gamma - 1} \left[\left(\frac{p_0}{p_i} \right)^{(\gamma-1)/\gamma} - 1 \right]} \tag{8}$$

Once the stagnation pressures are calculated, the data at a particular time during the test can be matched with the CFD simulations. Figure 7 shows results of two comparisons that agree well. In Fig. 7(b), the experimental data indicates the shock train is passing over four pressure taps while the CFD results predict only one normal shock. As discussed earlier, the pressure ratio before and after the shock(s) is the same.

Figure 8 shows comparisons between experimental, computational, and analytical methods for the Mach number and pressure distributions in the nozzle. The one-dimensional analytical solution has the lowest pressure ratio and highest Mach number in the constant area section because viscous effects are completely neglected. The two-dimensional numerical solution contains boundary layers on the wall, which effectively reduces the area ratio of the nozzle and causes the average Mach number to drop to about 1.95. The three-dimensional experimental Mach number drops even further (about Mach 1.85) due to the boundary layers
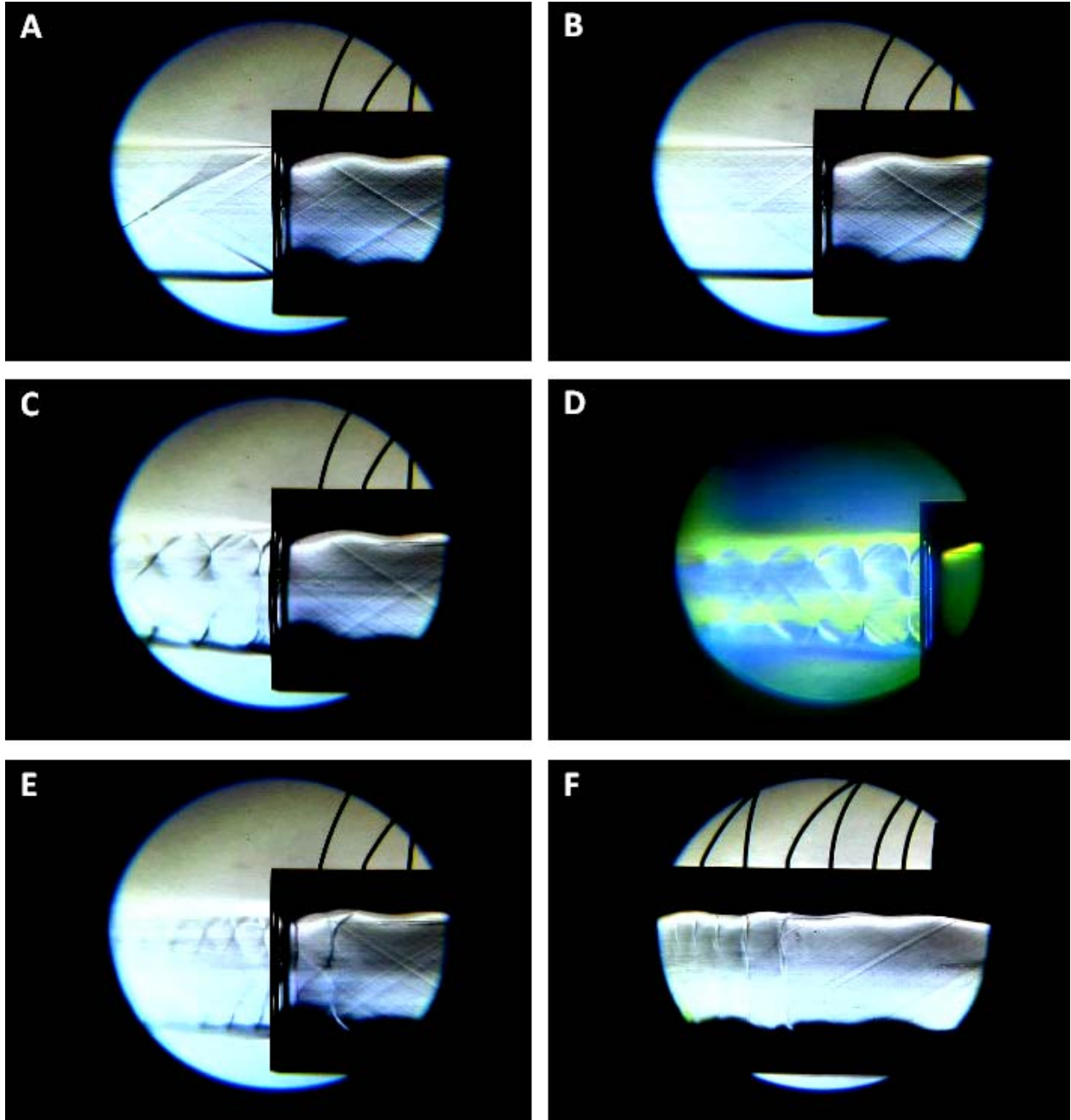
American Institute of Aeronautics and Astronautics

Figure 6. Schlieren photographs of different nozzle states.

American Institute of Aeronautics and Astronautics

(a) Comparison with $p_0 = 120$ kPa.
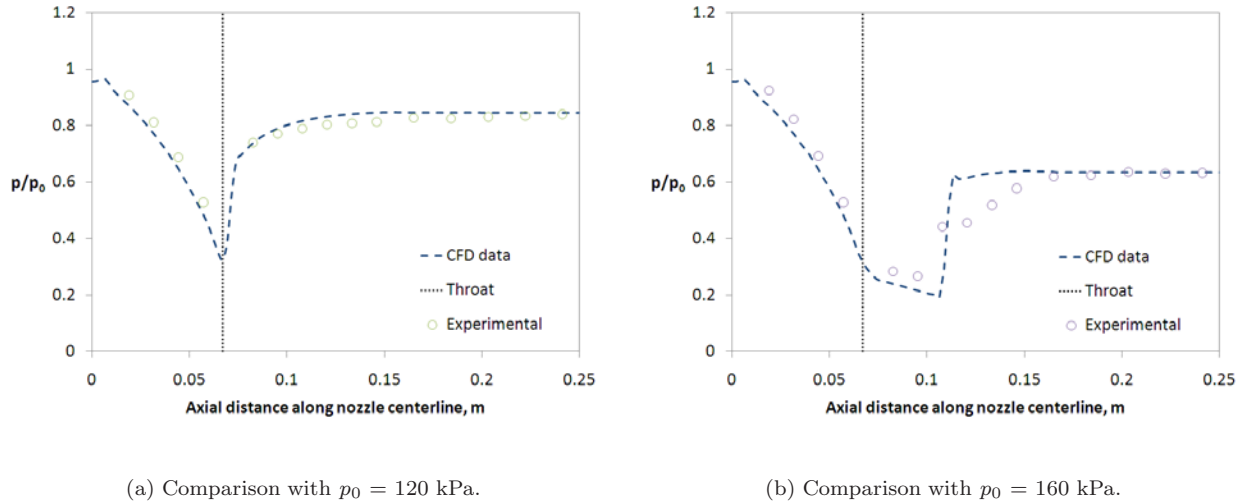

(b) Comparison with $p_0 = 160$ kPa.

Figure 7. Pressure comparison between computational and analytical solutions.

on all four walls. Even though the nozzle was designed for Mach 2.0 with a method that can be taught as part of an undergraduate compressible flow course, this result is intended to show students that limitations exist with inviscid solutions. As part of the final laboratory report, students are required to address several open-ended questions such as how to redesign the nozzle for exactly Mach 2.0 flow or how significant this problem becomes at the design Mach number is increased.

Another issue to address is the difference in how the CD nozzle is explained for this lab relative to textbooks. In the theory of most introductory texts, the backpressure is reduced to subsequently achieve each of the nozzle states. The flow is choked once $p/p_0 = 0.528$ at the throat, and consequently the mass flow rate remains the same as the backpressure is reduced further. Such an approach has occasionally caused confusion when students are presented with facilities that have a constant back pressure and variable stagnation pressure. The mass flow equation for choked flow is:

$$\dot{m}^* = A^* p_0 \sqrt{\frac{\gamma}{RT_0}} \left(\frac{2}{\gamma + 1} \right)^{(\gamma+1)/2(\gamma-1)} \tag{9}$$

It should be noted that once the flow is choked in this facility, p_0 and $\dot{m}^*$ are constantly changing during the test. Since the backpressure is not a parameter in the choked mass flow equation, it does not influence the flow so long as it is low enough for choking to occur.

III.   Discussion and Conclusions

In the authors' opinion, designing effective laboratory experiments for aerospace students can be difficult. A middle ground between cost, ease of operation, and suitable subject matter for junior-level students must be found. Along with being an enjoyable experience for the students, observations from these laboratories can be extended to related coursework. The validation and verification process across different analysis methods will likely be encountered by the students during their careers, and the aerodynamics laboratory is appropriate for introduce the approach (and so is the aero-structures laboratory). Along with low-speed wind tunnel experiments conducted in the same laboratory course, these laboratories provide a well-balanced introduction to experimental aerodynamics.
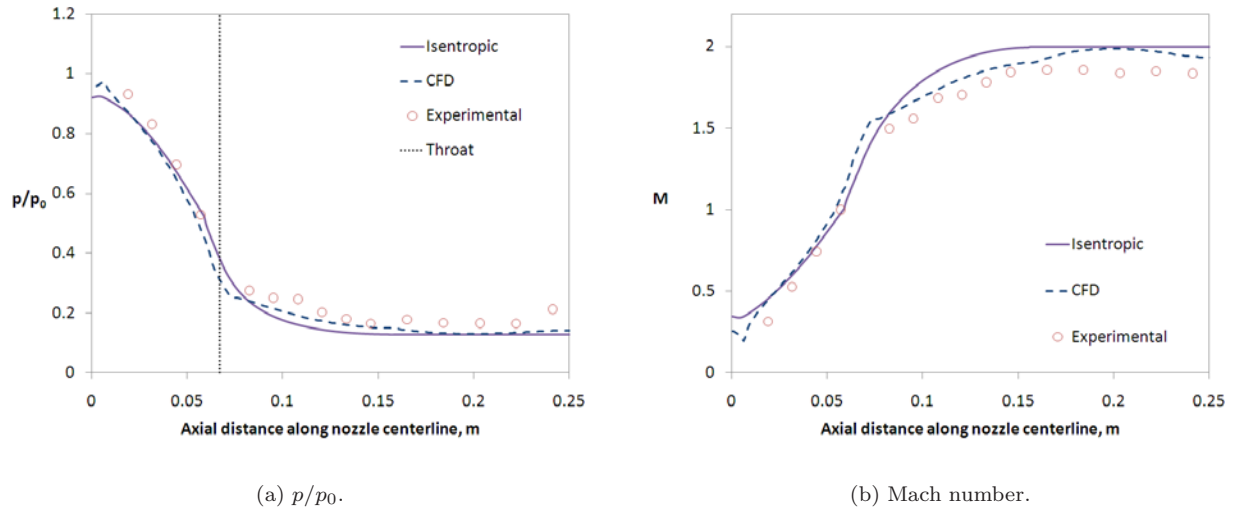
American Institute of Aeronautics and Astronautics

(a) p/p_0.

(b) Mach number.

Figure 8. Pressure ratio and Mach number comparison between experimental, computational, and analytical methods for perfectly expanded flow.

Acknowledgments

References

[1]Pierce A.J. and Lu, F.K., "Laser alignment method for portable schlieren system," *39th AIAA Fluid Dynamics Conference*, AIAA Paper 2009–3574, June 22–25, 2009, San Antonio, Texas.

[2]Pope A. and Goin, K.L., *High-Speed Wind Tunnel Testing*, Wiley, New York, 1965.

[3]Tannehill, J.C., Anderson, D.A. and Pletcher, R.H., *Computational Fluid Mechanics and Heat Transfer*, Taylor & Francis, Philadelphia, 1997.

[4]Shapiro, A.H., *The Dynamics and Thermodynamics of Compressible Fluid Flow*, The Ronald Press Company, New York, 1953.

American Institute of Aeronautics and Astronautics